Dalton Transactions

ROYAL SOCIETY OF CHEMISTRY

PERSPECTIVE

View Article Online
View Journal | View Issue

Cite this: *Dalton Trans.*, 2023, **52**, 12169

Management of typical VOCs in air with adsorbents: status and challenges

Qingqing Ye,[a,b] Yaoyao Chen,[a] Yizhao Li,[a] Ruiben Jin,[a] Qin Geng *[a] and Si Chen*[a,c]

The serious harm of volatile organic compounds (VOCs) to the ecological environment and human health has attracted widespread attention worldwide. With economic growth and accelerated industrialization, the anthropogenic emissions of VOCs have continued to increase. The most crucial aspect is to choose the appropriate adsorbent, which is very important for the VOCs removal. The search for environmentally friendly VOCs treatment technologies is urgent. The adsorption method is one of the most promising VOCs emission reduction technologies with the advantages of high cost-effectiveness, simple operation, and low energy consumption. One of the most critical aspects is the selection of the appropriate adsorbent, which is very important for the removal of VOCs. This work provides an overview of the sources and hazards of VOCs, focusing on recent research advances in VOCs adsorption materials and the key factors controlling the VOCs adsorption process. A summary of the key challenges and opportunities for each adsorbent is also provided. The adsorption capacity for VOCs is enhanced by an abundant specific surface area; the most efficient adsorption process is achieved when the pore size is slightly larger than the molecular diameter of VOCs; the increase in the number of chemical functional groups contributes to the increase in adsorption capacity. In addition, methods of activation and surface modification to improve the adsorption capacity for VOCs are discussed to guide the design of more advanced adsorbents.

Received 21st June 2023,
Accepted 11th August 2023

DOI: 10.1039/d3dt01930f

rsc.li/dalton

[a]*Yangtze Delta Region Institute (Huzhou), University of Electronic Science and Technology of China, Huzhou 313000, China. E-mail: chensi1003@zju.edu.cn, gengqin@csj.uestc.edu.cn*
[b]*Suzhou Industrial Technology Research Institute of Zhejiang University, Suzhou 215163, China*
[c]*College of Environmental Science and Engineering, Nankai University, Tianjin 300074, China*

1. Introduction

In recent decades, the ever-growing attention to environmental legislation has been paid for the emission control of VOCs as a consequence of increasing global awareness.[1] VOCs, characterized by their potential toxicity, carcinogenicity, and mutageni-

Yaoyao Chen

Yaoyao Chen is a postgraduate at the School of Chemical Engineering and Technology, Xinjiang University, and is currently undergoing combined training at the Yangtze Delta Region Institute (Huzhou) of the University of Electronic Science and Technology. Her current research interests include the application of carbon materials in energy storage and adsorption.

Yizhao Li

Dr Yizhao Li is currently a Special-Term Professor of Yangtze Delta Region Institute (Huzhou), University of Electronic Science and Technology of China (UESTC). He obtained his Ph.D. degree in Chemical Engineering from Xinjiang University in 2015. Then he worked as a Lecturer and Associate Professor in Xinjiang University from 2015 to 2021. He joined the UESTC in 2021. His research interests include carbon materials and nanocatalysts for energy storage and environmental purification.

city, are not only hazardous to human health but also harmful to the environment.[2] Long exposure to VOCs can lead to serious damage to the respiratory, nervous, and hemopoietic systems and even critical diseases including cancer and cardiovascular diseases. Moreover, it has been demonstrated that VOCs are the key precursors for the formation of photochemical smog, secondary aerosol, and ozone.[3,4] Therefore, the effective control of VOCs emission is becoming an increasingly vital issue around the world and still a long way off.

For now, the existing VOCs emission control methods are mainly divided into recycling and destruction methods. Recovery methods are primarily adopted for the VOCs waste gas with high concentration and recovery value, including methods of condensation, adsorption, absorption, and membrane separation.[5] Among them, adsorption receives widespread attention owing to its characteristics of cost-effectiveness, flexible operation, and low energy consumption. However, for most industrial source VOCs, actually, the destruction process including combustion, low-temperature plasma technology, photocatalysis, biological process, direct combustion, and catalytic combustion dominates, especially combustion.[6,7] It has been regarded as the mainstream treatment technology of VOCs waste gas because of its high treatment efficiency, ability to eliminate odor and low pollution. Worth mentioning is that adsorption and concentration prior to the industries emitting VOCs are characterized as low concentration and high air volume is of great importance for the combustion process to reduce operating load and costs, reduce energy consumption and ensure combustion treatment efficiency.[8,9] Apparently, adsorption plays a vital role in VOCs elimination in both recycling and destruction processes and deserves special attention.

Adsorbents are the key in VOCs adsorption technology, which directly determine the cost of investment, operation, and the safety of the process. It is expected in industrial application that an ideal absorbent possesses a large specific surface area, porosity and adsorption capacity and exhibits excellent selectivity for different gas adsorption, high mechanical strength, thermostability and easy regeneration. For this, number of adsorption materials have sprung out since ancient times, and activated carbon (AC) can be called the originator, which can be traced back to 400 B.C. Even now, ACs have the widest application for VOCs adsorption in varieties of scenarios.[10] Certainly, there also exist weaknesses in ACs such as high carbon loss, poor thermal stability, flammability and explosive nature.[11] Therefore, other carbon-based materials such as activated carbon fiber (ACF), charcoal, carbon nanotubes, and graphene were gradually developed.[5,12–15] At the same time, to achieve selective adsorption of VOCs, molecular sieves, a kind of important inorganic microporous material, were discovered. Depending on the aperture, they are classified as microporous molecular sieves (zeolite A, zeolites X and Y, β-zeolite, ZSM-5, MFI-zeolite, *etc.*), mesoporous molecular sieves (MCM, SBA, KIT, *etc.*) and hierarchical molecular sieves.[16,17] In the 1990s, metal organic frameworks (MOFs), a porous structure composed of metal ions and organic connectors, firstly came out, exhibiting excellent VOC adsorption performance. The last 20 years have witnessed the amazing development of MOFs, benefiting from their characteristics of huge specific surface area, multiple active sites and high and adjustable porosity.[18–20] There are thousands of MOFs now, containing a series of IRMOFs, MILs, ZIFs, UiO, *etc*. In addition, there also exist other new adsorption materials like hypercrosslinked polymeric resins (HPRs), minerals, magnetic nanoparticles, *etc*.

Except for the exploitation of new adsorbents, great efforts have also been paid to the modification of all kinds of adsorbents to optimize the adsorption performance, based on their respective features.[21–23] During this, it is of great necessity to understand the key factors controlling VOCs adsorption, which may guide to break through the bottlenecks of adsorption technology for industrial applications. The specific surface area, pore structures, and surface functional groups are proved to be the key ones, and their influences have been widely discussed these years.

This paper gives a comprehensive overview of the core work of adsorption technology used for VOCs elimination over the years, and critical emphasis will be given to the primary adsorption materials and their modification methods, as well as the discussion of the key factors controlling VOCs adsorption (Fig. 1). Furthermore, a critical overview regarding the challenges and opportunities for each adsorbent is proposed, along with some suggestions about future research aspects where efforts should be made. We hope to build a bridge between materials and VOCs adsorption performance for an in-depth understanding of the adsorption technology, providing guidance for the design of more advanced and excellent adsorbents.

Si Chen

Si Chen is currently an associate research fellow in the Yangtze Delta Region Institute (Huzhou), University of Electronic Science and Technology of China. She received her B.E. (2015) and Ph. D. degree (2020) from Hunan University and Zhejiang University, respectively. Her research interests focus on air pollution control technologies and environmental catalytic process, including plasma catalysis, adsorption of NO_x and volatile organic compounds.

2. Sources and hazards of VOCs

Due to differences in perspective or focus, different countries or organizations have different definitions of VOCs.[24] Even for the same country or organization, with the deepening of understanding and the advancement of practice, the definition

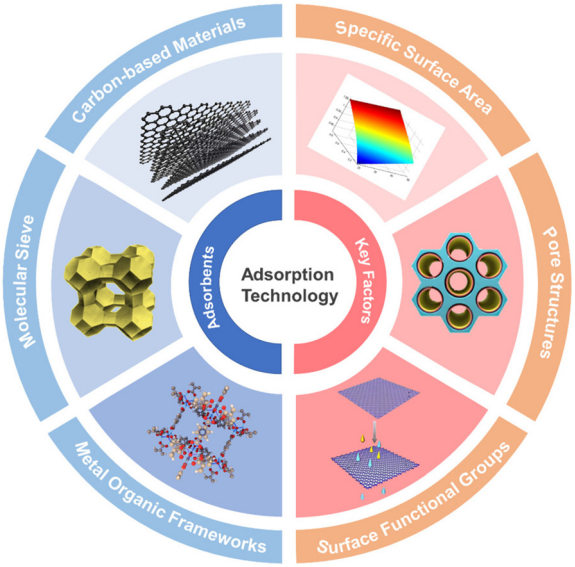

Fig. 1 Graphic outline of this review.

of VOCs has gone through a gradual process of improvement. The World Health Organization (WHO) defines VOCs as a type of organic compound that exists in the air as vapor at room temperature with a saturated vapor pressure exceeding 133.32 Pa and a boiling point between 50 °C and 260 °C. The definition of VOCs in the American Society for Testing and Materials (ASTM) standard ASTM D3960-1998 is any organic compound that can participate in atmospheric photochemical reactions. Unlike SO_2 and NO_x, which are relatively single sources, VOCs come from a wide and complex range of sources and can be mainly divided into natural and anthropogenic sources based on the different entities that generate VOCs.[25–27] Natural sources refer to VOC emissions caused by natural factors, which can be divided into biological emissions (emissions from vegetation, oceans, soil microorganisms, *etc.*) and non-biological process emissions (forest combustion and volcanic eruptions). Anthropogenic sources refer to VOC emissions caused by human activities, which can be roughly divided into industrial sources, transportation sources, domestic sources, *etc*. Among them, industrial sources account for the largest proportion of emissions, which mainly come from industries such as petrochemicals, coal chemical industry, basic chemical raw material manufacturing, furniture manufacturing, *etc*. From another perspective, the sources of VOCs can be further divided into indoor and outdoor sources. The common indoor sources mainly come from building and decorative materials, with formaldehyde and benzene derivatives being the most common, with formaldehyde accounting for the largest proportion, followed by xylene, toluene, and benzene. Outdoor sources mainly include various industrial exhaust gases and automobile exhaust generated by transportation.

Most VOCs have the common characteristics of low boiling point, high vapor pressure and strong photochemical reactivity. They are easily volatile at room temperature, characterized by a pungent odor, toxicity, flammability and explosion. From the perspective of VOCs' harm to the atmospheric environment, under the irradiation of ultraviolet light, the hydrocarbons contained in VOCs undergo a photochemical chain reaction with NO_x and SO_2 to generate secondary pollutants such as O_3, peroxyacetonitrate (PAN), aldehydes, and organic acids, which are emitted into the air with peculiar smell and odor. O_3 further oxidizes SO_2, NO_x, and VOCs in the atmosphere, generating anions such as SO_3^{2-} and NO_3^-, which combine with cations such as NH_4^+, Ca^{2+}, and Mg^{2+} in the atmosphere to form inorganic PM2.5. The primary pollutants formed by the direct emission of VOCs and the secondary pollutants formed by a series of reactions of VOCs can form photochemical smog in the air. In addition, VOCs will form highly active free radicals under light, and further reactions between highly active free radicals and other intermediate products with toluene, xylene, *etc*. will produce semi-volatile products. These semi-volatile products will then be distributed between the gas phase and the particle phase. Under suitable environmental conditions, semi-volatile organic compounds will enter the particle phase, causing an increase in particles. These generated particles are secondary organic aerosols.

In terms of the harm of VOCs to human health, long-term exposure can lead to death and serious chronic diseases. For example, benzene is highly toxic and carcinogenic. Its acute poisoning can lead to anesthesia, headache, dizziness, lethargy, and insanity. Toluene can affect the central nervous system, liver, kidneys, and skin. High concentrations of formaldehyde, widely used in industry, can cause nasopharyngeal carcinoma and damage cells and tissues.

3. Classification and modification of adsorbents

The adsorption method has the characteristics of high cost-effectiveness, flexible operation, and low energy consumption, and is considered one of the most promising VOC treatment technologies, with adsorbents being an important component. Therefore, the selection of adsorbents is the primary key issue to be solved in adsorption treatment technology. Generally, ideal adsorbents should have advantages such as large specific surface area and pore volume, more active adsorption sites, high thermal stability and chemical properties, large adsorption capacity, fast adsorption rate, and strong regeneration. At present, AC, zeolite molecular sieves, and MOFs are currently the mainstream VOC adsorption materials, especially AC, which is the most widely used adsorption material. Table 1 summarizes the performance, advantages and disadvantages of different VOC adsorption materials.

3.1 AC

AC is a porous carbon-containing material with a well-developed pore structure, large surface area, excellent chemical stability, rich functional groups, and other excellent physical

Table 1 Summary of the performance, advantages and disadvantages of different VOC adsorption materials

Type	Adsorbent	Adsorbate	S_{BET} (m^2 g^{-1})	V_{total} (cm^3 g^{-1})	Average pore size (nm)	Adsorption capacity (mg g^{-1})	Advantage	Disadvantage	Ref.
AC	Pine's pyrolytic carbon	2,4-Dichlorophenol	147.87	—	—	77.3	Large surface area, high porosity, abundant functional groups, stable chemical properties	Micropore-based, difficult for large molecule VOCs to enter, disordered pore structure increases diffusion resistance and prolongs adsorption equilibrium	31
	Shell activated carbon	1,1,1-Trichloro ethane	902	—	—	93.1			32
	Shell-activated carbon	*p*-Cresol	140.02	0.0787	2.2	32.77			33
	Coal-based activated carbon	Methane	426.49	0.217	5.86	28.96			34
	Polyacrylonitrile/ cellulose nanocrystal nanofibers	Methyl ethyl ketone	3497	2.62	11.02	184.2			36
	Pitch-based carbon fibers	Chloroform vapor	1985	0.988	12.6	1040			37
	Pitch-based carbon fibers	Tetrachloroethylene	800	0.474	—	396			38
	Wheat straw-based biochar	Toluene	312.62	0.2218	1.34	73.63			39
	Bagasse-based biochar	Acetone	78.15	0.1448	—	110.1			41
	KOH-activated carbon	Benzene	3100	2.08	2.68	2035.8			43
	Bamboo-based biochar	Acetone	10.2	—	—	71.6			44
	Hickory-based biochar	Toluene	289	—	—	57.3			44
	Bone-based biochar	Toluene	1405.06	0.97	0.68	288.12			45
	Wood based carbon	Ammonia vapor	1807	—	2.1	136			47
	Coal-based activated carbon	Ammonia vapor	1081	—	0.85	148			47
	Coal-based activated carbon	Phenanthrene	1770.49	0.99	—	125			50
	Activated carbon fibers	*p*-Nitrophenol	1413	0.69	1.95	350			51
	Activated carbon fibers	Acetaldehyde	2170	1.01	—	160			52
	Cork stoppers-based carbon	Acetone	2060	0.75	2.2	1250			53
Zeolites molecular sieve	Y/ZSM-5	Toluene	557	0.269	—	135	Adjustable specific surfaces area and pore structures, good thermal stability, easy modification of surface	Hydrophilicity and greatly susceptible to water vapor, limited adsorption capacity, high costs of preparation	54
	NaY@CoO	Isopropanol	861.446	0.387	10	189			55
	USY-3-0.2 M (alkali modification)	Butyl acetate	845.0	0.60	30–40	219			56
	Y@St-DVB-12 h	Toluene	470	0.162	7–9	118.3			57
	Y zeolite pellet	Toluene	779	0.52	—	254.4			58
MOFs	MIL-101(Cr)	*n*-Pentane *n*-Hexane *n*-Heptane	4293	2.43	0.98	181.42 98.15 82.65	High specific surface area, larger pore diameter, high selectivity, good dispersibility, reusability	Low mechanical strength, high cost, solid powder, poor stability of water	59
	MIL-100	Methanol	1567	1.54	3.11	161			60
	UiO-66	Dichloromethane	980	0.59	7–12	510.3			61
	Bio-MOF-11	Toluene	580	0.35	0.51–3.77	42.4			62

properties, which can be in full contact with gases or impurities, thereby giving specific powerful adsorption performance for the adsorption of VOCs.[28–30] In general, AC can be divided based on raw materials such as biomass AC (the precursors are wood chips,[31] walnut shells,[32] coconut shells,[33] *etc.*), coal-based AC (the precursors are anthracite coal[34] and lignite[35]) and AC fibers (the precursors are polyacrylonitrile,[36] intermediate phase asphalt,[37] phenolic resin,[38] *etc.*). The preparation process mainly consists of carbonization and activation. Carbon materials can be used for the selective adsorption of VOCs by adjusting the pore structure and controlling the surface functional groups during the adsorption process.[39] The high adsorption capacity and selectivity of porous carbon are closely related to the large specific surface area, suitable pore structure, abundant surface functional groups, and adsorption sites. In particular, the micropores are the main adsorption sites for VOCs, while the mesopores provide transport channels for the diffusion of VOCs.[5]

3.1.1 Biomass-AC. Biomass carbon material is a carbon-rich material that is usually thermochemically transformed at less than 700 °C and exhibits higher carbon yields, particularly at slow pyrolysis rates.[40] Renewable biomass and biomass waste are considered to be promising precursors for AC, which is widely used for the treatment of pollutants, including inorganic and organic pollutants, as well as pesticides and antibiotics.[41] The adsorption performance of biomass carbon is closely related to its specific surface area and pore size structure, as well as to the type of biochar and pyrolysis conditions.[42,43] Zhang *et al.*[44] evaluated the adsorption performance of 15 different biomass carbon prepared from five common raw materials including bamboo (BB), sugarcane bagasse (BG), Brazilian pepper wood (BP), sugar beet tailings (BT) and hickory wood (HW) through gas phase adsorption experiments. AC synthesized under slow pyrolysis at 300–600 °C was used for the adsorption of VOCs with adsorption capacities ranging from 5.58 to 91.2 mg g^{-1} (Fig. 2a).

The adsorption capacity of biomass-AC is related to the combined effect of its surface area and non-carbonated organic matter (NOM) content. Biochar with high pyrolysis temperature and large specific surface area is mainly based on physical adsorption, while biochar with low pyrolysis temperature and small specific surface area is based on a partitioning mechanism (Fig. 2b). Kaikiti *et al.*[46] synthesized a series of bio-based porous carbons from four fruit sources (pomegranate peels (PB), prickly pear peels (PPB), carob bean gum (CB) and locust bean gum (LBGB)) by slow pyrolysis (350 °C and 550 °C). The adsorption performance of four volatile organic compounds (VOCs), consisting of cresols, dimethyl trisulfide (DMTS), hexane, and benzene, was systematically and comprehensively compared. The doping of heteroatoms (*e.g.*, O, N, and S) is effective in improving the surface chemistry of AC. In particular, AC containing nitrogen functional groups (*i.e.*, N-doping) can achieve a significant increase in the adsorption capacity. Yang *et al.*[45] prepared a series of N-doped biomass porous carbons from three types of food waste (bones, crab shells, and shrimp shells) by pyrolysis at 400–900 °C with a

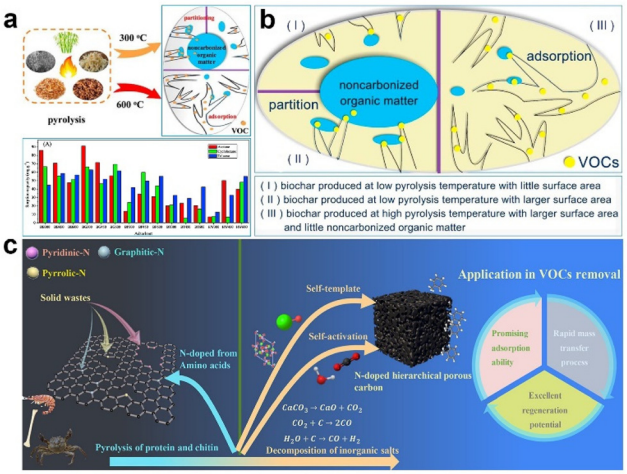

Fig. 2 (a) Adsorption performance and mechanism of VOCs onto different biomass-AC,[44] Copyright 2017, Elsevier. (b) Schematic diagram of combined effect of surface area and NOM on VOC sorption by biochar,[44] Copyright 2017, Elsevier. (c) Synthesis of HPC and N-doped HPC from food waste components (bone, protein, and chitin) for VOC adsorption,[45] Copyright 2022, Elsevier.

rate of 10 °C min^{-1}. The pyrolysis process is divided into two stages: the pyrolysis of proteins and the thermal decomposition of inorganic salts (Fig. 2c). Several gaseous products (CO_2 and H_2O) are released during the pyrolysis of proteins to form abundant micropores. As the pyrolysis temperature increases, inorganic salts begin to decompose to produce CO. In addition, the inorganic salts can be used as pore-forming templates and activators. The bone-derived biomass porous carbon has a large specific surface area (1405.06 m^2 g^{-1}) and high pore volume (0.97 cm^3 g^{-1}), exhibiting an adsorption performance of 288.12 mg g^{-1} for toluene and an adsorption rate of 0.189 min^{-1}.

In summary, biomass charcoal is available from a wide range of sources and still has great potential for application in VOC adsorption due to its excellent adsorption efficiency and low cost. In addition, biochar has a number of drawbacks, including flammability, easy clogging of pores, and hygroscopicity. The production of biochar may release environmentally harmful VOCs. As the adsorption process of VOCs on biochar is very complex, further studies on the adsorption process and mechanism are needed to promote the application of biochar in volatile organic compound emission reduction.

3.1.2 Coal-based AC. Coal-based AC is prepared from anthracite, petroleum coke, lignite, and other coal resources with high-temperature carbonization and activation to obtain AC with a large specific surface area and high porosity.[47] Modified AC from abundant coal resources is expected to be an efficient adsorbent for VOCs. AC as an adsorbent has not only physical adsorption, but also chemisorption, and its chemisorption is mainly due to its surface having a certain amount of surface chemical functional groups.[41] The main component of anthracite is carbon, which is predominantly aromatic in composition and can be converted directly into

carbon material under the right conditions. Zhang *et al.*[48] prepared coal-based activated carbon (CAC) for the removal of cyclic volatile methylsiloxanes (cVMSs) from waste leachate using a one-step process with anthracite coal as the raw material. cVMSs are hydrophobic volatile organic pollutants. When CAC is added to water, cVMSs tend to move on the surface and inside the CAC. Zheng *et al.*[49] prepared three different AC using low-rank bituminous coal as the raw material by the KOH activation method. The adsorption experiments on methane under high pressure revealed 313.15 K as the critical temperature point for methane adsorption. Below the critical temperature, the adsorption capacity decreases rapidly with increasing temperature. Xiao *et al.*[50] activated anthracite coal by the microwave activation method for the adsorption of polycyclic aromatic hydrocarbons (PAHs). The effects of microwave activation time, AC dosage, and other factors on the adsorption performance were investigated, indicating that the AC prepared by the microwave activation method had a better removal effect on phenanthrene.

Coal-based AC with a reasonable pore structure, good adsorption performance, high mechanical strength, and the advantage of recyclability is used as a VOC adsorbent. In addition, anthracite can be activated and fired at high temperatures to form columnar or honeycomb microporous AC with large specific surface area and low resistance through different processes. The use of coal is more limited due to its complex composition and the ease of secondary pollution caused by handling ash.

3.1.3 Activated carbon fibers. Activated carbon fibers (ACFs) are another form of AC; they have unique properties compared to AC and exhibit a well-arranged fiber structure. In addition, ACFs can be made into the desired formats, such as paper cloth, fabric, felt/carpet and other shapes.[51] The raw materials used in the preparation of ACFs are usually synthesized from different materials (polyacrylonitrile, bitumen, phenolic resin, *etc.*) through high temperature (700–1000 °C) carbonization and activation. Fig. 3a shows a schematic diagram of electrostatic spinning technology. A mixture of a polymer and functional material is usually mixed under magnetic stirring and ultrasound to obtain a homogeneous spinning solution.[36] The spun fibers are then collected on a roller under pressure and the influence of an electrostatic field. The ACFs are obtained after a series of treatments (pre-oxidation/carbonization and activation). In contrast to AC, ACFs have a thin fiber shape combined with short and straight microporous pore channels, giving them faster adsorption kinetics and mass transfer rates (Fig. 3b). Therefore, ACFs can be excellent adsorbents for the adsorption of VOCs.

PAN is the most commonly used polymer precursor for electrostatic spinning due to its high melting point, which can be oxidized into a thermally stable conjugated structure while retaining its original shape. PAN-based fibers are ideal precursors for ACF preparation due to their flexibility and the ability to adjust the strength and modulus of the fibers by controlling the carbonization temperature. Awad *et al.*[36] prepared PAN/cellulose nanocrystalline fibers with uniform diameter distribution. The resulting nanofibers have a large specific surface area of 3497 $m^2 g^{-1}$ and high pore volume of 2.62 $cm^3 g^{-1}$. The adsorption capacities of methyl ethyl ketone and cyclohexane are up to 1.7 and 1.8 g g^{-1}, respectively (Fig. 4a and b). Apart from the PAN, pitch with low cost and high carbon content can also be used as a precursor for fibers. Yue *et al.*[37] prepared ACFs with low cost and high adsorption performance using isotropic pitch as the raw material by melting and blowing, air stabilization, N_2 carbonization and CO_2/H_2O activation (Fig. 4c). The obtained ACFs are typical microporous adsorbents with a large specific surface area of 1000–2000 $m^2 g^{-1}$ and high microporous volume of 0.435–0.715 $cm^3 g^{-1}$. They have a strong adsorption affinity for chloroform vapor, and the adsorption capacity was 1004 mg g^{-1} at 22 °C. In addition, the adsorption capacity of ACFs can be improved by modifying

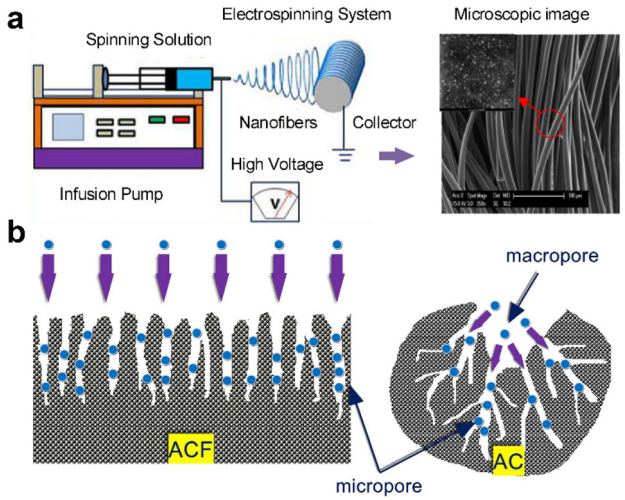

Fig. 3 (a) Schematic diagram of electrostatically spun fibers,[30] Copyright 2020, Elsevier. (b) Diagram of the adsorption mechanism of VOCs by ACFs,[5] Copyright 2017, Elsevier.

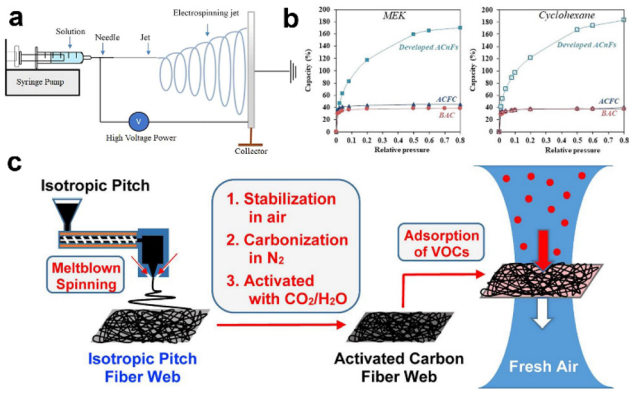

Fig. 4 (a) Schematic diagram of the electrostatic spinning device,[36] Copyright 2021, Elsevier, and (b) MEK and cyclohexane adsorption isotherm of PAN-CNC ACNFs, ACFC, and BAC,[36] Copyright 2021, Elsevier. (c) Schematic diagram of the process of adsorption of VOCs by ACFs,[37] Copyright 2017, Elsevier.

them for VOCs. Metal oxide nanocrystalline aerogels have been reported to be used as effective adsorbents for a variety of oxidized VOCs compared to AC, and these materials exhibit higher adsorption capacities. Recently, Baur *et al.*[52] developed an efficient adsorbent combining ACFs with alkali metal oxides (CaO, La_2O_3, ZnO, MgO, and Al_2O_3). Compared to unmodified ACFs, this adsorbent provides up to 10 times the amount of acetaldehyde adsorbed. The results show that the metal oxide modification improves the affinity of ACFs for polar VOCs due to the introduction of surface oxygen groups.

In short, the microporous structure of ACFs is more conducive to VOC adsorption than AC. The specific surface area and porosity of carbon fibres can be regulated by an activation process, which increases the surface area and porosity. ACFs are naturally hydrophobic and have a small number of chemical functional groups on the surface, which facilitates the adsorption of non-polar or weakly polar volatile organic compounds. Notably, the application of ACFs in practical industry is limited due to the high cost of fiber precursors and their associated processing costs.

The disadvantages of AC affect its ability to adsorb VOCs. AC is a naturally non-polar adsorbent, which inevitably limits the adsorption of hydrophilic VOCs. In addition, the porous structure of AC is mainly in the microporous range (less than 2 nm), which hinders the access of VOC molecules, especially those with larger molecular sizes, into the pores. More importantly, the disordered pore structure of ACs increases the diffusion resistance and prolongs the adsorption equilibrium.

3.2 Zeolite Molecular sieves

Zeolite Molecular sieves, with features to sieve molecules at molecular size based on their unique and highly ordered pore structures, have been widely used for VOCs adsorption.[63,64] Though they exhibit a much smaller specific surface area and poorer adsorption capacity than other adsorption materials, extremely uniform and controlled pores can be designed and accessible only from molecular sieves; therefore, it facilitates the selective adsorption of VOCs. Zeolites are the typical microporous molecular sieves including zeolite A, zeolites X and Y (faujasite type), β-zeolite, and ZSM-5, and the attention of researchers is primarily focused on the regulation of the Si/Al ratio and hydrophobic modification for greater adsorption–desorption of VOCs.[65–68] Guvenc *et al.*[69] found that the adsorption site of MTBE on ZSM-5 was mainly concentrated at the pore intersection (Fig. 5a and b), while the Al element in ZSM-5 would promote the adsorption of water molecules, thereby creating a competitive relationship to inhibit the adsorption of organic pollutants (Fig. 5c). The Si/Al ratio of zeolites greatly affects the adsorption performance of VOCs, especially when water is present. Bhatia *et al.*[70] analyzed the influence of the Si/Al ratio on the adsorption capacity and found that the presence of water vapor would greatly inhibit the adsorption of ethyl acetate by silver-loaded Y molecular sieves (Si/Al = 40), but a bare effect was observed for AgZSM-5 molecular sieves with high silicon–aluminum ratio (Si/Al = 140). As claimed by Wang *et al.*,[68] there was a large

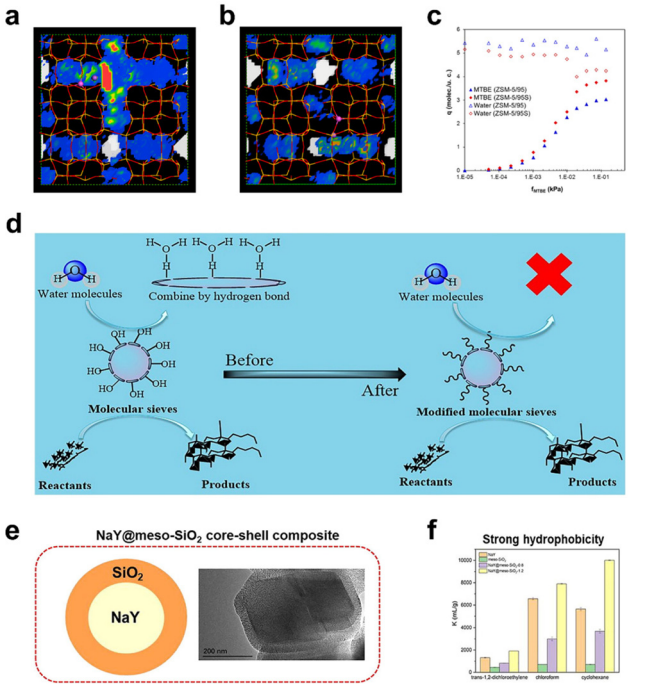

Fig. 5 MTBE and water density fields in (a) ZSM-5/95 and (b) ZSM-5/95S at the maximum MTBE loading. MTBE density field is in white, and water density increases from blue (near-zero density) to red. Aluminum atoms and sodium cations are represented as pink and purple spheres, respectively. Straight and sinusoidal channels run in the vertical and horizontal directions, respectively. (c) Comparison of MTBE and water adsorption capacity of ZSM-5/95 and ZSM-5/95S as a function of MTBE fugacity. Water fugacity is constant at 3.5 kPa.[69] Copyright 2012, ACS. (d) The diagram of the effect of hydrophilic Si–OH on the catalytic performance of molecular sieves.[68] Copyright 2021, Elsevier. (e) The schematic diagram of the prepared NaY@meso-SiO_2 core–shell composites; (f) the hydrophobicity of zeolite before and after modification.[73] Copyright 2022, Elsevier.

amount of hydrophilic Si–OH on the surface of molecular sieves, which would easily combine with H_2O, avoiding the adsorption of VOCs (Fig. 5d). Hence, hydrophobic modification is always a research priority, and the commonly used strategies are silanization modification, dealuminization, acid treatment, *etc.*[68] Kremer *et al.*[71] synthesized the ultrastable Y molecular sieve (USY) with good hydrophobic properties by skeleton dealumination removal of Y zeolite. Zhang *et al.*[72] modified NaY molecular sieves by TMCS (a silane reagent), leading to the increase of water contact angle from 0 to 69.2°, and the toluene adsorption capacity was enhanced by 78% at a relative humidity of 80%. Liu *et al.*[73] coated mesoporous SiO_2 with different shell thicknesses on the surface of NaY and formed a NaY@meso-SiO_2 core–shell composite, as displayed in Fig. 5e and f, which significantly improved the hydrophobicity of NaY zeolite and the diffusion of VOCs.

The bottleneck of zeolites is the large gas diffusion resistance due to the smaller pores, resulting in evident difficulty in desorption.[16,74] Then, an era of ordered mesoporous materials came out along with the first synthesis of MCM-41

in 1992,[75] followed by the development of a series of mesoporous materials like MCM-*n*, SBA-*n*, KIT-6, MSU-*n*, FDU-*n*, *etc*.[76–78] Tuning surface functional groups, morphology and different origin of silicon sources are the main concerned aspects of this field. To avoid the competitive occupation of adsorption sites between water molecules and toluene molecules, as shown in Fig. 6a–c, Yu *et al.*[79] functionalized MCM-48 by the co-condensation method, which presented excellent dynamic toluene adsorption capacity under both dry conditions (194.62 mg g^{-1}) and 20% RH (122.42 mg g^{-1}). Zhou *et al.*[80] developed amino-functionalized spherical mesoporous silica (ASMS) *via* an easy 3-aminopropyltrimethoxysilane (APTES) treatment, showing great toluene adsorption capacity (98.1 mg g^{-1}) and outstanding regenerability by thermal desorption. Liu *et al.*[81] reported phenyl modified KIT-6 with much better toluene selective adsorption and a far better hydrophobicity (Fig. 6d and e), which can be attributed to the conjugated π-electron effect between the aromatic rings of phenyl groups and toluene molecules within the mesoporous channels.

In the nearest ten years, the hierarchical molecular sieves spring up. It is a new composite containing different levels of channels connected to each other, which not only maintains the characteristics and advantages of each level of pores, but also produces synergistic effects through coupling, exhibiting better performance than traditional porous sieves containing only one grade of pore structure.[83–86] Currently, researchers focus on the adjustment of the pore characteristics by changing the preparation conditions, the type and dosage of the template agent, and alkali treatment to obtain good performance materials. Feng *et al.*[82] etched the USY zeolite by NaOH and NH_4HF_2 to remove part of non-framework Al and Si, and the obtained material contains a large number of both micropores and macropores, showing evidently increased toluene adsorption capacity (Fig. 6f–h). Han *et al.*[87] introduced a water-soluble polyacrylamide (PAM) hydrogel into the SAPO-34 synthesis system and prepared hierarchical SAPO-34 with both micropores and mesopores, whose catalytic life is prolonged by about three times with highly enhanced adsorption performance. Jiang *et al.*[88] reported meso–microporous ZSM-5 by hydrothermal synthesis, and excellent adsorption and desorption performance (the adsorption capacity is up to 47.02 mg g^{-1}), water resistance (the adsorption capacity decreased only 4.64%), and renewability (the adsorption and desorption efficiency are up to 95% and 97%, respectively) were achieved.

In a word, from the discovery of original natural zeolites to the development of a large number of new synthetic zeolites, from microporous crystalline aluminosilicate molecular sieves to ordered mesoporous materials and microporous materials, and to hierarchical molecular sieves, the optimization of pore structure and adsorption capacity for the zeolite molecular sieve has progressed with marvellous rapidity. Meanwhile, the hydrophobicity has also been greatly improved contributed by the ingenious modification methods. Attention in the future should be paid to the enhancement of cycle stability and regeneration performance, super stability in different rugged environments, and operating economy, to better serve the adsorption, catalysis and separation of VOCs.

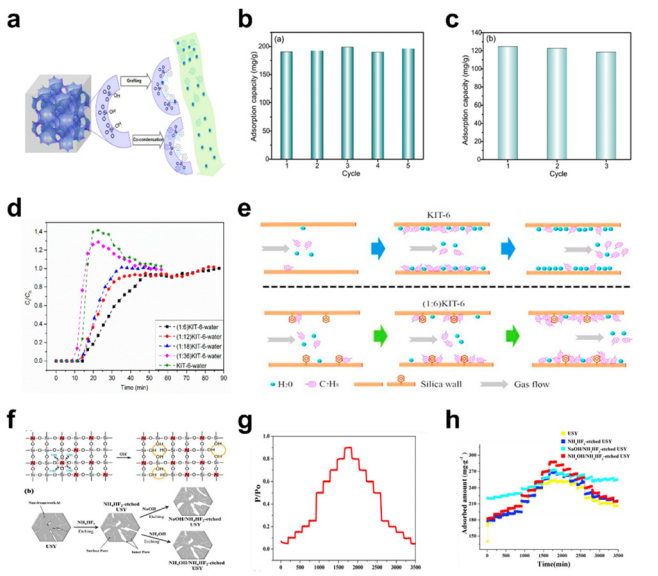

Fig. 6 (a) Schematic diagram of toluene adsorbed on MCM-48 adsorbents functionalized *via* different methods under wet conditions; adsorption cycle of co-M48(1 : 5)-100/48: (b) RH = 0 and (c) RH = 20%,[79] Copyright 2022, Springer. (d) The breakthrough curves of toluene adsorption (100 ml min^{-1} N_2 gas flow with 1000 ppm toluene; 0.1 g sample with 40–60 mesh; adsorbent bed diameter: 6 mm, length: 15 mm; 60% RH at 25 °C); (e) the schematic diagram of the dynamic adsorption process.[81] Copyright 2018, Elsevier. (f) Schematic diagram of the modification of USY by NH_4HF_2 + NaOH or NH_4HF_2 + NH_4OH solution; (g) and (h) toluene adsorption amount–time curves of different USY samples under different pressure conditions,[82] Copyright 2019, Elsevier.

3.3 MOFs

MOFs are organic–inorganic hybrid materials with periodic network framework structures formed by self-assembly of metal ions or metal clusters and organic ligands, which are developed from coordination chemistry. It is worth noting that by selecting matching organic ligands, the structure of MOFs can be flexibly controlled.[89] MOF materials have attracted the attention of many scholars since their birth in the 1990s.[90] After nearly 30 years of research, scientists' enthusiasm for MOF materials has not abated; their ever-changing structure and potential properties make them one of the research hotspots in chemistry and materials science. The MOF-1 (Cu (4,4′-bpy)$_{1.5}$·NO_3(H_2O)$_{1.25}$(4,4′-bpy)) with an adamantane type network structure was synthesized by O. M. Yaghi *et al.* with 4,4′-bipyridine and $Cu(NO_3)_2$·$2.5H_2O$.[91] In 1999, a landmark MOF-5 [92] using terephthalic acid and Zn^{2+} was synthesized with a pore size distribution concentrated at 8 Å and a Langmuir specific surface area of up to 3917 m^2 g^{-1}, far exceeding conventional materials such as AC and molecular sieves. Owing to their high specific surface area, adjustable pore structure, numerous controllable functional groups, and large-scale production characteristics, MOFs have unique

application prospects in many fields such as energy storage, electrochemical reactions, sensors, biomedicine, and especially VOC adsorption. In recent years, the technology of controlling and managing VOCs based on MOF materials has gradually emerged as a rising star, and MOFs have become a promising class of microporous VOC adsorption materials.

Various types of MOFs have been synthesized, including IRMOFs, ZIF series, MIL series and UiO series, for the treatment of VOCs. IRMOF materials are the most representative MOF materials and have a regular branching structure, which endows them with a large specific surface area and high porosity. Several typical IRMOFs, such as MOF-5, IRMOF-3, MOF-199, and so on, were prepared.[93] The most studied one is MOF-5, which is a three-dimensional MOF with a simple cubic structure constructed by a solvothermal method using a rigid organic ligand terephthalic acid (BDC) and a transition metal Zn. Yaghi *et al.* (Fig. 7a).[92] have found that the saturated adsorption capacity of MOF-5 for VOCs such as dichloromethane, chloroform, benzene, and hexane can reach 1211, 1367, 802, and 703 mg g^{-1}, respectively. Through further research, they found[93] that the adsorption capacity of MOF-74 and MOF-199 for tetrahydrothiophene, benzene, dichloromethane, and ethylene oxide was one order of magnitude higher than that of Calgon BPL AC, with a maximum of 59 times. The ZIF series is a tetrahedral framework material mainly synthesized by the reaction of imidazole ligands (Ims) with Co(II) or Zn(II). Boudjema *et al.*[94] conducted a sorption capability experiment on commercial ZIF-8 and found that it would preferentially adsorb *n*-hexane, with a saturated adsorption capacity of 250 mg g^{-1}. Xie *et al.*[95] prepared amino functionalized ZIF-8 with many microporous structures and functional groups, which endow it with outstanding VOC adsorption performance. Its maximum adsorption capacities for aniline, benzene, and toluene are 245.31, 185.68, and 207.49 mg g^{-1}, respectively (Fig. 7b and c). The MIL series has strong flexibility, high water stability, and good selectivity. Among them, MIL-53, MIL-100, and MIL101 are the most representative, and have received widespread attention. Tehrani *et al.*[96] prepared hierarchical micro–mesoporous MIL-101(Cr), which exhibited 235.3 ± 0.05 and 291.6 ± 0.04 wt% adsorption efficiency for benzene and toluene, respectively. Therefore, MIL-101 can be used as an efficient adsorbent and has broad application prospects in the adsorption and removal of VOCs. In addition, the UiO series of MOF materials also enriches the classification. Zhao *et al.*[97] synthesized defective UiO-67 by changing the amount of benzoic acid. When the molar ratio of Zr^{4+} to benzoic acid is 1 : 10, there are more adsorption sites, higher benzoic acid content, stronger π–π stacking, and excellent adsorption diffusion behavior in the 67-ben-10 sample, and the sample exhibits the maximum adsorption capacity for toluene, which is 480 mg g^{-1}. Vellingiri *et al.*[98] compared the adsorption of toluene by different types of MOFs under environmental conditions. As shown in Fig. 7d, the order of equilibrium adsorption capacity of all MOFs is ZIF-67 (224 mg g^{-1}) > UiO-66 (166 mg g^{-1}) > MOF-199 (159 mg g^{-1}) > MIL-101 (98.3 mg g^{-1}). The maximum adsorption capacity of ZIF-67 is attributed to the maximum specific surface area (1401 m^2 g^{-1}).

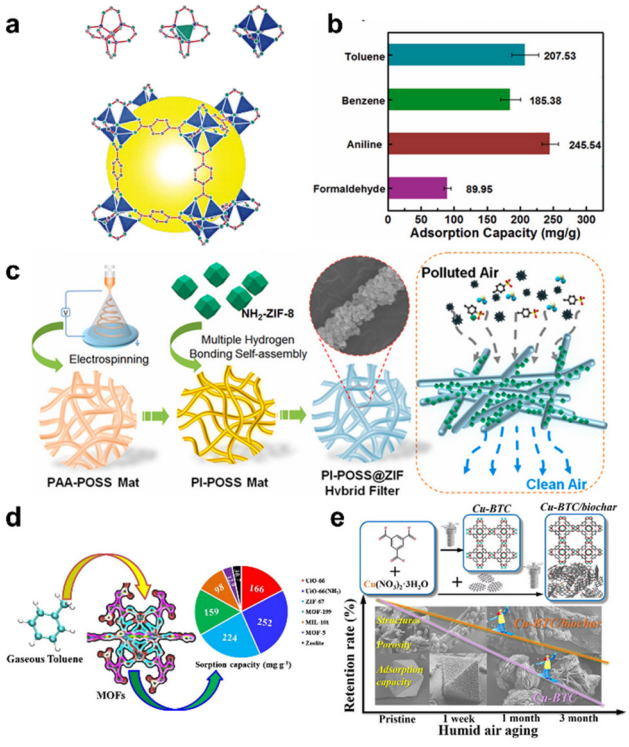

Fig. 7 (a) Construction of the MOF-5 framework,[92] Copyright 1999, Springer Nature. (b) The adsorption capacity of PI-POSS@ZIF for different VOCs. (c) Schematic illustration for the fabrication process of the PI-POSS@ZIF hybrid mat,[95] Copyright 2021, Elsevier. (d) The adsorption of toluene by different types of MOFs under environmental conditions,[98] Copyright 2017, Elsevier. (e) The capacity decay process of Cu-BTC increases with humid air aging,[99] Copyright 2023, Elsevier.

Even so, there are still some drawbacks of MOFs as VOC adsorbents. VOCs in the environment usually coexist with gaseous water molecules (humidity). In addition, water vapor in industrial flue gas is about 10%. Most MOF materials are highly sensitive to water, which not only harms the crystallinity of MOFs but may also cause hydrolysis of metal–organic bonds, leading to final structural collapse and porosity loss. In addition, humidity significantly inhibits the adsorption of VOCs by MOFs, mainly through competitive adsorption between gaseous water molecules and VOC molecules. Zhang *et al.*[99] found that the adsorption capacity of Cu-BTC for toluene significantly decreased by 28.5% after exposure to air. And as the exposure time prolongs, its adsorption capacity for toluene continuously decreases. After 3 months of humid air aging, the crystal structure of Cu-BTC collapsed. Meanwhile, with the degradation of the internal structure of Cu-BTC, its pore structure is severely damaged, and the BET surface area retention rate is less than 40% (Fig. 7e). Therefore, how to solve the above shortcomings is important for MOFs as VOC adsorbents. Dong *et al.*[100] designed a novel bimetallic MOF PCN-250 (Fe_2Co) to improve MOFs' humidity tolerance. Performance testing found that for dry acetone gas with a flow

rate of 160 min g^{-1}, the adsorption capacity of PCN-250 (Fe_2Co) was 355 mg g^{-1}. When the gas humidity increases to RH = 40%, about 93% of the acetone capture capacity is still retained, indicating that MOF adsorbents have good tolerance to the humidity of acetone vapor. In addition, PXRD measurements show that PCN-250 (Fe_2Co) also exhibits good stability towards VOCs. The enhanced adsorption performance is partly attributed to the introduction of open Co(II) sites, and the adsorption mechanism is different under humid and dry conditions, as calculated by DFT. Since water molecules are more likely to adsorb on metal sites under humid conditions, the H atoms of H_2O^* adsorbed on Co(II) atoms subsequently attack O_3 first to form free radicals, which improves the performance of adsorption and catalysis; however, this is not a general strategy.

In summary, the huge specific surface area, adjustable pore structure and remarkable physicochemical properties of MOFs make their adsorption performance superior to that of traditional adsorbents, which are one of the most promising adsorbents for VOCs at present. However, the expensive cost and poor water resistance of MOF materials limit their widespread industrial applications. Although their stability and selectivity can be adjusted by hydrophobic modification, they are still not advantageous in practical applications.

4. Key factors and removal mechanism of VOCs adsorption

4.1 Key factors of VOCs adsorption

Adsorption is regarded as one of the most promising VOCs treatment technologies owing to its characteristics of cost-effectiveness, flexible operation, and low energy consumption. However, drawbacks like limited adsorption capacity, difficulty in regeneration, high replacement cost, and susceptibility to environmental factors especially water vapor, dust, *etc*. still limit the industrial application of adsorption. How does one break through these bottlenecks from the perspective of special design of adsorbing materials? Analyzing and extracting the key factors controlling VOCs adsorption are considered as the top priority. It is widely reported that it is the specific surface area, pore structure and surface functional groups that primarily affect the adsorption performance of adsorbents. Therefore, understanding and adjusting these key factors are the focus courses in the present research.

4.1.1 Specific surface area and pore structure. The specific surface area is one of the crucial factors for adsorption materials, directly determining their performance of VOCs adsorption. Often, the larger, the better. It is demonstrated that the adsorption capacity of VOCs exhibits a good linear relationship with the specific surface area of materials and pore volume.[42,103] On the basis of this, designing and synthesizing new adsorbents with increasing surface area is always a hot topic. From the primary molecular sieve with an average specific surface area of 800 m^2 g^{-1}, hypercrosslinked polymeric resin (average specific surface area of 1225 m^2 g^{-1}), AC (average specific surface area of 1404 m^2 g^{-1}), to MOFs (average specific surface area of 2653 m^2 g^{-1}), it is seen that the specific surface area of adsorbents is continuously iterating and updating, along with the new discovery of adsorption materials. Certainly, this research is continuing.

Recently, the Yang Kun group[104] reported MOF-177 prepared by the solvent thermal method, whose Langmuir and BET specific surface area are 4170 m^2 g^{-1} and 2970 m^2 g^{-1}, respectively, showing excellent adsorption capacity for several VOCs like acetone, benzene, toluene, ethylbenzene, *o*-xylene, *m*-xylene, *etc*. Fig. 8a displays the MIL-101 with a specific surface area of 3891 m^2 g^{-1} reported by Jhung *et al.*,[101] which exhibited a huge benzene adsorption capacity of 1303 mg g^{-1} and rapid adsorption rate of 5.15 mg g^{-1} s^{-1} at 30 °C and pressure of P/P_0 = 0.5 (Fig. 8b and c). Another way to increase the surface area of adsorbents is to activate them by types of gases (air, water vapor, CO_2, *etc*.) at a certain temperature and pressure, or chemical reagents like strong acids, alkaline hydroxides and salts, which has been widely studied for ACs. Liu *et al.*[105] obtained the ACs with a specific surface area of 3708 m^2 g^{-1} *via* the activation treatment by KOH. Jain *et al.*[102] prepared a type of mesoporous AC

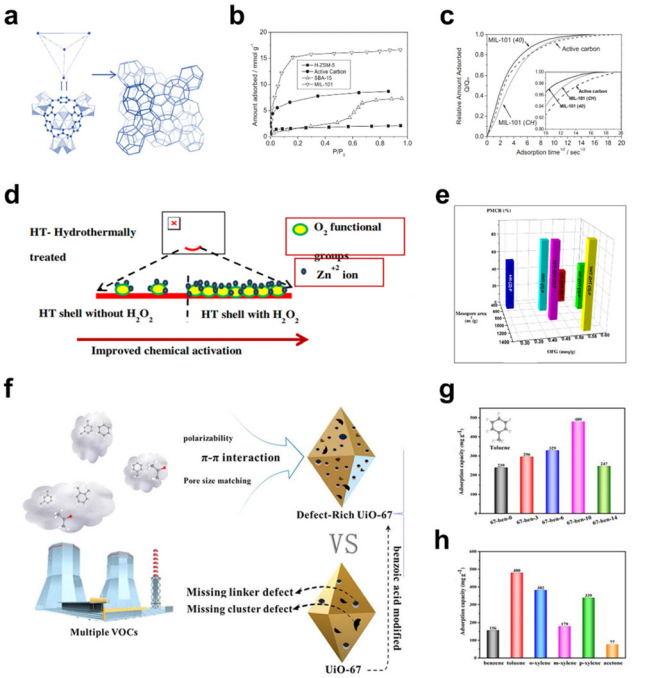

Fig. 8 (a) Schematic of the crystal structure of MIL-101. Each intersection of the schematic structure (right) corresponds to a supertetrahedron built up of trimers of chromium octahedra and terephthalate moieties (left); (b) sorption isotherms of benzene at 30 °C on MIL-101(40), a commercial active carbon, HZSM-5 zeolite, and mesoporous silica SBA-15; (c) sorption kinetics of benzene on MIL-101(40), MIL-101(CH), and active carbon at 30 °C in the vapor phase. The inset shows the sorption kinetics near equilibrium for clarity,[101] Copyright 2007, Wiley. (d) Schematic of the improved chemical activation process; (e) PMCR (percentage molasses color removed) of AC prepared under different pretreatment conditions as a function of mesopore area and OFG,[102] Copyright 2015, Elsevier. (f) Comparation of the defective UiO-67 and origin UiO-67; the adsorption capacity of the 67-ben-10 benzene series for (g) the defective UiO-67 and (h) UiO-67.[97] Copyright 2022, Elsevier.

with a specific surface area of 2450 m^2 g^{-1} by incorporating H_2O_2 as an oxidizing agent during hydrothermal pre-treatment of the raw material (coconut shell), and claimed that the specific surface area of ACs is seriously dependent on the ratio of activators (Fig. 8d and e).

Except for specific surface area, pore structure properties like pore size and shape also play a vital role for VOCs adsorption. As for pore size, there are four types: macropores (>50 nm), mesopores (2–50 nm), micropores (<2 nm) and narrow micropores (<1 nm), the first three of which approximately correspond to HPR, zeolite, MOFs and ACs, respectively. In particular, hierarchical molecular sieves or ACs containing both micropores and mesopores have been developed these years as previously discussed. Then, how does one select the most suitable adsorbent for the adsorption of the target VOCs? It has been verified that it is the most effective adsorption process when the pore diameter is slightly larger than the molecular diameter of VOCs. When the pore size is far larger, the pore would be just like a channel showing extremely week adsorption force between the material and VOCs molecules, and thus reduce the adsorption performance. As studied by Crespo,[106] the carbon nanotubes with a pore size of 1.2 nm and 1.68 nm were employed for the adsorption of benzene and cyclohexane, and the 1.2 nm one exhibited greater VOC adsorption capacity. Since most VOC molecules are on the micropore or even narrow micropore-scale, micropores are usually considered as the primary adsorption sites for VOC adsorption. It is reported by Lillo-Ródenas *et al.*[107] that toluene can be adsorbed both in the micropores and narrow micropores, and emphasized that the volume of narrow micropores is just the controlling factor for its adsorption, especially at low concentration. However, materials with only micropores or even narrow micropores have been verified to be not the optimum. Notably, the diffusion of VOCs is equally important during their adsorption process, and mesopores can just fit to this procedure. Tsai *et al.*[108] analyzed and calculated the adsorption kinetic curve of several VOCs molecules adsorbed on ACs, and concluded that the diffusion coefficient of VOCs in mesopores can be about three orders of magnitude higher than in micropores. Zhao *et al.*[97] developed a strategy to optimize both the adsorption sites and diffusion behavior of UiO-67 by changing the amount of benzoic acid in the precursor solution, and the obtained defective UiO-67 achieved a toluene adsorption capacity of 480 mg g^{-1} (Fig. 8f–h). Mechanism study showed that the adsorption performance was related to the polarizability of the VOC molecules, the method of pore entry and the molecular size.

Based on the above discussion, it is clear that the specific surface area and the pore structure exhibit a combined effect on the adsorption performance of materials, which is a dialectical process and greatly dependent on the character and structure of the targeted VOC molecules.

4.1.2 Surface functional groups. The type and number of functional groups on the surface of AC are also key factors affecting the adsorption capacity of VOCs.[5] The surface functional groups on the surface heteroatom (O, N, S, and halogen) can effectively improve the surface chemical properties of AC. The oxygen and nitrogen groups on AC are considered to be the most significant adsorption types.

Oxygen functional groups are divided into three types: acidic, neutral and basic functional groups. Carboxylic acids are formed by liquid phase oxidation, while hydroxyl and carbonyl groups are formed by gas phase oxidation. These oxygen-containing functional groups are more inclined to adsorb polar VOCs by forming hydrogen bonds.[5,110] The amount of adsorption of polar compounds is affected by the number of oxygen-containing groups. Usually the carboxyl and hydroxyl groups show strong electronic absorption capacity. Adsorption of benzene is mainly caused by the formation of an electronic complex between the carboxyl group (acidic group) and the benzene ring, which firmly binds the benzene ring to the surface of the adsorbent through hydrogen-bonding interactions with oxygen-containing functional groups.[42] Fig. 9 shows the relationship between the adsorption capacity and the number of functional groups for benzene and methanol. Among them, the relative adsorption coefficient of benzene (0.98152) is higher than that of methanol (0.95638). There is a linear relationship between the saturation sorption amount and the number of chemical functional groups. As the number of functional groups increases, the saturation sorption of VOCs also increases. An *et al.*[109] explored the enhanced adsorption effect of various functional groups on the surface of the carbon model and the optimal adsorption position of polar formaldehyde molecules in the AC model through a mathematical modeling system. The results showed that the adsorption of formaldehyde by the carboxyl group consists of two main parts: the first part of the carboxyl group and the formation of hydrogen bonds with formaldehyde; the second part can only be adsorbed by the weaker van der Waals forces. As the carboxyl groups would adsorb multiple layers of formaldehyde, the adsorption force on the outer formaldehyde molecules gradually weakened, accompanied by the appearance of desorption. However, its overall adsorption effect is significantly stronger than that of several other functional groups studied. Zhao *et al.*[111] investigated the effect of oxygen-containing functional groups on the competing adsorption mechanisms of non-polar benzene molecules and polar water mole-

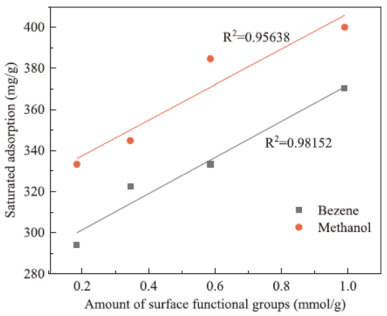

Fig. 9 Relationship between adsorption capacity and the amount of surface functional groups,[42] Copyright 2020, Elsevier.

cules on the surface of carbon materials. It was determined that the carboxyl group has a strong influence on the hydrophilicity of the carbon material. The ether group will release adsorption space for benzene adsorption on the surface of the carbon material, facilitating the adsorption of benzene.

Nitrogenous functional groups are mainly available through pyrolysis of nitrogen-containing compounds (organic: melamine and urea; inorganic: ammonium oxalate; nitrogenous macromolecules and nitrogenous biomass: proteins, chitin, and microalgae). NH_3 treatment is another common method of introducing nitrogen-containing functional groups, both to increase the amino-N group and to increase the nitrogen content of biochar. Xu *et al.*[53] recovered the cork wine stopper and prepared it into a VOC adsorption material through ammonia activation, which contained rich amino functional groups and showed good adsorption capacity for acetone, toluene and benzene.

4.2 Removal mechanism of VOC adsorption

4.2.1 Removal mechanism of AC. Density functional theory (DFT) can give useful insights into the mechanism and nature of the interaction of the VOCs with the AC. Sharafinia *et al.*[116] successfully synthesized a set of AC adsorbents prepared from leguminous plant particles. The carbon atoms around the porous sites as well as the oxygen atoms of the AC have negative potentials. This means that the latter position is the most favorable region for electrophilic attack. The hydrogen atoms of the hydroxyl group and the dangling hydrogen atoms located at the edge of the AC have positive potentials, suggesting that these sites may interact with nucleophiles. DFT calculations show that the adsorption of VOCs on AC occurs by charge transfer from VOCs to AC, and the VOC molecules preferentially adsorb on the defective sites of AC with negative values of adsorption energy and Gibbs free energy change. Meng *et al.*[117] prepared lignin-based ACFs by the electrospinning method for VOC removal. The large specific surface area and microporous structure of the adsorbent contribute to adsorption, while the role of chemical functional groups is related to the polarity of VOCs. For single-component dynamic adsorption, the molecular polarity of VOCs plays a crucial role in the adsorption process. For multicomponent adsorption, methanol and acetone prefer to be adsorbed on the polar groups on the surface of the adsorbent through dipole–dipole interactions, and the adsorption process is physisorption. Guo *et al.*[118] developed a facile strategy to modify AC by the mixture of siloxane with long and short chains. Water has the highest E_{ads} (−0.16 eV) on the OH-modified carbon layer through hydrogen bonding interactions. Therefore, the adsorption of water precedes the adsorption of ethanol, ethyl acetate or toluene on the carbon layer. E_{ads} on the carbon layer modified by Si showed that the synergistic effect of hydrogen bonding interactions between the adsorbed molecules and the –OH group of Si increased the adsorption energy for ethanol, ethyl acetate, toluene and water. In particular, the E_{ads} values for ethanol and ethyl acetate (−0.81 and −0.77 eV) were higher than that for water (−0.73 eV). This indicates that the adsorption of ethanol and ethyl acetate is predominant on the silica-modified carbon layer (Fig. 10). The main adsorption sites for toluene can be transferred to the inner regions of the carbon layer. However, water molecules are still present only on the boundary of the carbon layer. The number of adsorption sites in the inner region of the carbon layer is larger than in the boundary region. It can be concluded from the DFT analysis that siloxane modification can improve the selectivity of AC to VOCs.

4.2.2 Removal mechanism of zeolites. It has been widely proved that DFT is an effective way to shed light on the adsorption mechanism at the molecular level. Yin *et al.*[55] studied the typical VOC adsorption by metal (Ni, Co, Cu, and Mn)–oxide nanoparticle loaded NaY zeolite, and DFT results showed that the interaction of metal–oxides with isopropanol (E_a = −0.72 eV) and acetone (E_a = −0.699 eV) is greater than that with toluene (E_a = −0.177 eV) due to their oxygen functional groups (the coexistence of coordination bonds and hydrogen bonds); thus, NaY@CoO exhibited excellent adsorption performance for isopropanol (189 mg g^{-1}) and acetone (124 mg g^{-1}) under RH = 50%, much higher than toluene. Besides, VOCs can just adsorb on NaY by weak van der Waals forces (E_a = 0.042–0.073 eV), while the loading of metal–oxides enhances the adsorption ability of VOCs and the strong competitive adsorption between water molecules and VOC molecules is greatly reduced, making the adsorption capacity of NaY@M_xO_y for VOCs significantly improved under high humidity conditions. For better guidance of the design of adsorbents, Hessou *et al.*[112] systematically investigated the interaction between sodium-exchanged faujasite Y zeolite and a large set of VOCs by DFT calculations. It is found that styrene presents the strongest interaction with NaY zeolite (130 kJ mol^{-1}), while

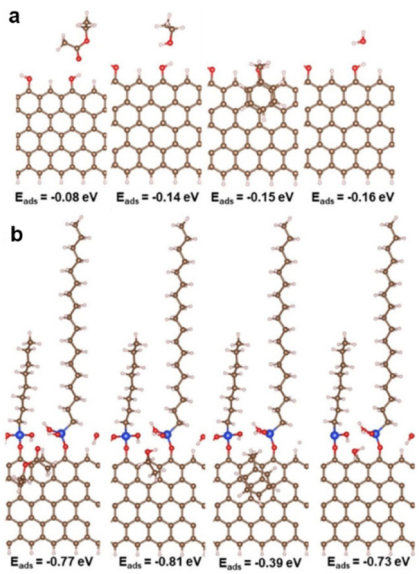

Fig. 10 Adsorption geometries of ethanol, ethyl acetate, toluene and water by (a) OH-modified and (b) Si-modified carbon layers,[118] Copyright 2021, ACS.

methane the weakest (25 kJ mol^{-1}), indicating that this type of zeolite may be unsuitable for methane adsorption.

In addition, *in situ* diffuse reflectance Fourier transform infrared spectroscopy also provides a way to take a closer look at the molecular mechanism of adsorption. Kang *et al.*[113] analyzed the adsorption of gaseous DCM and water vapor on FAU and MFI zeolites, as shown in Fig. 11a. Compared with the spectra of gaseous DCM, the peaks (757 and 742 cm^{-1}), assigned to the asymmetric and symmetric stretching vibrations of the C–Cl bond, exhibit no shift on all the zeolites, indicating that the C–Cl bond is relatively independent and barely influenced by the surface of the adsorbent. However, the peaks around 3200–3100 cm^{-1} (stretching vibrations of C–H bonds) exhibit an evident red-shift in both cases, suggesting that the C–H bond of DCM is weakened or elongated when the molecule is adsorbed on the surface of the solid. In addition, the disappearance of the peak around 1267 cm^{-1} (rocking vibrations of the two H atoms) is observed when DCM is adsorbed on FAU zeolites, along with the appearance of a new peak from 1199 to 1055 cm^{-1}, implying that the rocking vibrations of the two H atoms of DCM are constrained by the pore space. Thus, it is supposed that DCM should be in intimate contact with the surface of FAU zeolites *via* an H atom, while for MFI zeolites, both of the peaks remain, indicating that DCM is relatively free in the middle of the pores in MFI zeolites without strong interaction with the pore walls (Fig. 11b).

4.2.3 Removal mechanism of MOFs. MOF materials exhibit efficient adsorption performance in VOC removal due to their large specific surface area, abundant tunable porosity, and open metal sites. However, MOFs with different compositions and structures have different bonding ways to different types of VOCs, resulting in different reaction mechanisms.[114] In summary, when there are no special functional groups in VOC molecules, such as aliphatic-VOCs, they tend to rely on non-specific adsorption, such as van der Waals forces. At this time, the adsorption performance is mainly determined by the pore structure of MOFs, and is accompanied by poor selectivity. When aromatic ring functional groups exist in VOC molecules, adsorption is often dominated by stronger π–π host–guest interactions. At the same time, the ligand molecules of MOFs are also required to have a large number of aromatic groups to selectively adsorb such VOCs. When the polar functional groups are present in the molecules of VOCs, the variation of the types of polar functional groups shows different reaction mechanisms, such as hydrogen bonding interactions, electrostatic interactions, acid–base interactions, and unsaturated metal coordination interactions. For example, VOC molecules containing functional groups such as N, O or F usually rely on hydrogen bonding interactions. If the VOCs with N or O-functional groups have certain acid–base properties, and electrostatic interactions, acid–base interactions may become dominant; the adsorption of VOCs containing sulphur is more inclined to interact with unsaturated soft metals. For gases with more complex compositions, the selectivity and adsorption capacity of MOFs may be impaired, especially by water vapour. Moisture can adsorb and occupy the adsorption sites in the structure of MOFs, thus reducing the adsorption of VOCs. Meanwhile, moisture tolerance can be improved by hydrophobic modification.[115] However, the adsorption of VOCs by MOFs is still a complex process, and thus the adsorption process and mechanism need to be further investigated by using *in situ* characterization techniques and DFT calculations.

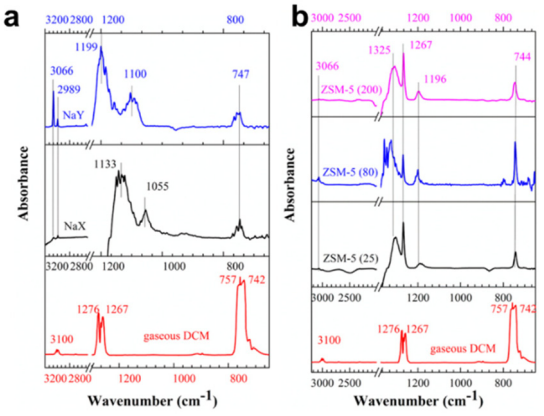

Fig. 11 *In situ* DRIFTS spectra of DCM on FAU (a) and MFI zeolites (b) compared with the spectrum of gaseous DCM at a temperature of 30 °C.[113] Copyright 2018, ACS.

5. Conclusions and perspectives

This review focuses on VOC pollution control technology and provides a detailed introduction to three typical adsorption materials as VOC adsorbents, including AC, molecular sieves, and MOFs. Relevant insights and modification methods for improving adsorption capacity, regeneration performance, and susceptibility to environmental factors have been proposed. And the factors that affect the adsorption performance of adsorbents, namely specific surface area, pore structure, and surface functional groups, were elaborated in detail. However, there is still a significant gap between the practical application and experimental research of adsorbents in real emission environments and many issues need further research.

(1) Although the large surface area and pore volume of AC adsorbents have a positive effect on the adsorption capacity of VOCs, the use of ACs for large-scale applications at the industrial level still presents certain challenges: (i) incomplete desorption will affect the lifetime and regeneration cost of the AC due to irreversible adsorption. The material design should consider not only the high adsorption capacity, but also the regeneration capacity of the adsorbent as well as its accessibility. (ii) The flammability of ACs may cause fires, especially during exothermic adsorption. (iii) The high permeability, pore resistance and hygroscopicity of AC limit its wide application in VOC treatment. (iv) The detailed mechanism of

adsorption conditions in the adsorption process for AC adsorption of VOCs needs to be more refined.

(2) Zeolite molecular sieves are a big family containing micropores, mesopores, and hierarchical pores, and it is the rapid development of the adjustable pore structure and specific surface area that gives zeolites excellent adsorption capacity for VOCs. However, the hydrophilicity of most molecular sieves limits their practical industrial applications, since H_2O would preferentially adsorb and occupy the sites, avoiding the adsorption of VOCs. Thus, hydrophobic modification is an eternal topic for all types of zeolites and great advances have been made through silanization modification, dealumination, acid treatment, surface functional group tuning, *etc*., but hardly sufficient. Further research is also required to further enhance the tolerance in the presence of moisture. In addition, even though some of the zeolites have been commercialized, developing high-quality mesoporous or hierarchical zeolites through more cost-efficient and environment-friendly synthesis methods needs to be investigated in upcoming works. Notably, during the practical applications, it is appealed that the cycle stability and regeneration performance, and super stability in different rugged environments of zeolites are urgently needed, which were concerned in few studies. Attention in the future should be paid more on those issues, to better serve the adsorption, catalysis and separation of VOCs.

(3) MOFs have a tunable pore structure and excellent physicochemical properties, making them promising VOC adsorbents for research. On the one hand, the high preparation cost of MOF materials limits their practical application as adsorbents. How to industrialize and commercialize MOF materials is one of the key factors determining the future development of MOF materials. On the other hand, the MOF structure must be carefully designed, and suitable inorganic (nodes) and organic ligands (linkers) must be selected to construct special MOFs for specific applications; subsequently, the changes of selectivity and adsorption capacity of MOFs must be tested under the coexistence of various volatile organic compounds; another key point is to solve the problem of stability of MOFs under humid conditions. However, compared to the many research results that have been reported so far, there are still very limited MOF materials that can really achieve high adsorption efficiency, which remains a challenge.

Conflicts of interest

The authors declare no competing financial interest.

Acknowledgements

This work was supported by "Pioneer" and "Leading Goose" R&D Program of Zhejiang (no. 2023C03017), the National Natural Science Foundation of China (grant no. 22225606, 22261142663 and 22202032), Zhejiang Provincial Natural Science Foundation of China (grant no. LQ23B070011 and LZY23B030007), Key R&D Project of Xinjiang (2022B02031) and S&T Special Program of Huzhou (2022ZD2066).

References

1 X. Lyu, H. Guo, Y. Wang, F. Zhang, K. Nie, J. Dang, Z. Liang, S. Dong, Y. Zeren and B. Zhou, *Chemosphere*, 2020, **246**, 125731.
2 L. Cheng, W. Wei, A. Guo, C. Zhang, K. Sha, R. Wang, K. Wang and S. Cheng, *J. Cleaner Prod.*, 2022, **379**, 134919.
3 E. Berezina, K. Moiseenko, A. Skorokhod, N. V. Pankratova, I. Belikov, V. Belousov and N. F. Elansky, *Atmosphere*, 2020, **11**, 1262.
4 X. Zhang, S. Gao, Q. Fu, D. Han, X. Chen, S. Fu, X. Huang and J. Cheng, *Environ. Sci. Pollut. Res.*, 2020, **27**, 28853–28866.
5 X. Zhang, B. Gao, A. E. Creamer, C. Cao and Y. Li, *J. Hazard. Mater.*, 2017, **338**, 102–123.
6 M. Zang, C. Zhao, Y. Wang and S. Chen, *J. Saudi Chem. Soc.*, 2019, **23**, 645–654.
7 S. Chen, H. Wang and F. Dong, *J. Hazard. Mater.*, 2022, **427**, 128150.
8 C. Yang, G. Miao, Y. Pi, Q. Xia, J. Wu, Z. Li and J. Xiao, *Chem. Eng. J.*, 2019, **370**, 1128–1153.
9 T. Hyodo and Y. Shimizu, *Anal. Sci.*, 2020, **36**, 401–411.
10 A. A. Abd, M. R. Othman and J. Kim, *Environ. Sci. Pollut. Res.*, 2021, **28**, 43329–43364.
11 M. Basso and A. Cukierman, *Ind. Eng. Chem. Res.*, 2005, **44**, 2091–2100.
12 M. A. Sidheswaran, H. Destaillats, D. P. Sullivan, S. Cohn and W. J. Fisk, *Build. Environ.*, 2012, **47**, 357–367.
13 L. Wei, L. Zhuang, Z. Shao-peng, J. Wei-wei and M. Dan-zhu, *J. Fuel Chem. Technol.*, 2021, **49**, 861–872.
14 S. Wang, Z. Chen, Y. Cai, X.-L. Wu, S. Wang, Z. Tang, B. Hu, Z. Li and X. Wang, *Environ. Funct. Mater.*, 2023, DOI: **10.1016/j.efmat.2023.03.001**.
15 Y. Sun, X. Liu, M. Zhu, Z. Zhang, Z. Chen, S. Wang, Z. Ji, H. Yang and X. Wang, *DeCarbon*, 2023, **2**, 100018.
16 L. Zhi, W. Jianying, W. Yong, Z. Xiangjing, G. Chunlei, N. Yuanfeng and L. Huan, *Chin. J. Chem. Eng.*, 2020, **14**, 2211–2221.
17 W. Gao, X. Tang, H. Yi, S. Jiang, Q. Yu, X. Xie and R. Zhuang, *J. Environ. Sci.*, 2023, **125**, 112–134.
18 N. Stock and S. Biswas, *Chem. Rev.*, 2012, **112**, 933–969.
19 J. Fonseca, T. Gong, L. Jiao and H.-L. Jiang, *J. Mater. Chem. A*, 2021, **9**, 10562–10611.
20 B. Kim, Y.-R. Lee, H.-Y. Kim and W.-S. Ahn, *Polyhedron*, 2018, **154**, 343–349.
21 C. Martínez and A. Corma, *Coord. Chem. Rev.*, 2011, **255**, 1558–1580.
22 Z. Li, Y. Jin, T. Chen, F. Tang, J. Cai and J. Ma, *Sep. Purif. Technol.*, 2021, **272**, 118659.
23 Y. Lv, S. Wu, N. Li, P. Cui, H. Wang, S. Amirkhanian and Z. Zhao, *J. Cleaner Prod.*, 2023, **385**, 135633.

24 V. Vaishnav, P. Patel and N. Patel, *Thin Solid Films*, 2005, **490**, 94–100.
25 A. Kansal, *J. Hazard. Mater.*, 2009, **166**, 17–26.
26 Y. M. Kim, S. Harrad and R. M. Harrison, *Environ. Sci. Technol.*, 2001, **35**, 997–1004.
27 B. Huang, C. Lei, C. Wei and G. Zeng, *Environ. Int.*, 2014, **71**, 118–138.
28 W. K. Pui, R. Yusoff and M. K. Aroua, *Rev. Chem. Eng.*, 2019, **35**, 649–668.
29 I. I. Laskar, Z. Hashisho, J. H. Phillips, J. E. Anderson and M. Nichols, *Sep. Purif. Technol.*, 2019, **212**, 632–640.
30 L. Zhu, D. Shen and K. H. Luo, *J. Hazard. Mater.*, 2020, **389**, 122102.
31 Y. Song, Y. Wang and R. Han, *Environ. Sci. Pollut. Res.*, 2023, **30**, 31294–31308.
32 R. R. Bansode, J. N. Losso, W. E. Marshall, R. M. Rao and R. J. Portier, *Bioresour. Technol.*, 2003, **90**, 175–184.
33 Y. Zhu and P. Kolar, *J. Environ. Chem. Eng.*, 2014, **2**, 2050–2058.
34 B. Zhang, P. Liu, Z. Huang and J. Liu, *ACS Omega*, 2023, **8**, 10303–10313.
35 A. Arami-Niya, T. E. Rufford and Z. Zhu, *Carbon*, 2016, **103**, 115–124.
36 R. Awad, A. H. Mamaghani, Y. Boluk and Z. Hashisho, *Chem. Eng. J.*, 2021, **410**, 128412.
37 Z. Yue, A. Vakili and J. Wang, *Chem. Eng. J.*, 2017, **330**, 183–190.
38 Z. Yue and A. Vakili, *J. Mater. Sci.*, 2017, **52**, 12913–12921.
39 X. Zhang, W. Xiang, X. Miao, F. Li, G. Qi, C. Cao, X. Ma, S. Chen, A. R. Zimmerman and B. Gao, *Sci. Total Environ.*, 2022, **827**, 153996.
40 P. D. Dissanayake, S. You, A. D. Igalavithana, Y. Xia, A. Bhatnagar, S. Gupta, H. W. Kua, S. Kim, J.-H. Kwon, D. C. W. Tsang and Y. S. Ok, *Renewable Sustainable Energy Rev.*, 2020, **119**, 109582.
41 H. Rajabi, M. H. Mosleh, T. Prakoso, N. Ghaemi, P. Mandal, A. Lea-Langton and M. Sedighi, *Chemosphere*, 2021, **283**, 131288.
42 X. Li, L. Zhang, Z. Yang, P. Wang, Y. Yan and J. Ran, *Sep. Purif. Technol.*, 2020, **235**, 116213.
43 X. Liu, H. Zhu, W. Wu, D. Lin and K. Yang, *J. Hazard. Mater.*, 2022, **424**, 127355.
44 X. Zhang, B. Gao, Y. Zheng, X. Hu, A. E. Creamer, M. D. Annable and Y. Li, *Bioresour. Technol.*, 2017, **245**, 606–614.
45 Y. Yang, C. Sun, Q. Huang and J. Yan, *Chemosphere*, 2022, **291**, 132702.
46 K. Kaikiti, M. Stylianou and A. Agapiou, *Bioresour. Technol.*, 2021, **342**, 125881.
47 W. H. Lee and P. J. Reucroft, *Carbon*, 1999, **37**, 21–26.
48 C. Zhang, S. Jiang and W. Zhang, *Environ. Sci. Pollut. Res.*, 2018, **25**, 4803–4810.
49 Y. Zheng, Q. Li, C. Yuan, Q. Tao, Y. Zhao, G. Zhang, J. Liu and G. Qi, *Fuel*, 2018, **230**, 172–184.
50 X. Xiao, F. Tian, Y. Yan, Z. Wu, Z. Wu and G. Cravotto, *Korean J. Chem. Eng.*, 2015, **32**, 1129–1136.
51 D. Tang, Z. Zheng, K. Lin, J. Luan and J. Zhang, *J. Hazard. Mater.*, 2007, **143**, 49–56.
52 G. B. Baur, I. Yuranov and L. Kiwi-Minsker, *Catal. Today*, 2015, **249**, 252–258.
53 X. Xu, Y. Guo, R. Shi, H. Chen, Y. Du, B. Liu, Z. Zeng, Z. Yin and L. Li, *Appl. Surf. Sci.*, 2021, **565**, 150550.
54 S. Wu, Y. Wang, C. Sun, T. Zhao, J. Zhao, Z. Wang, W. Liu, J. Lu, M. Shi, A. Zhao, L. Bu, Z. Wang, M. Yang and Y. Zhi, *Chem. Eng. J.*, 2021, **417**, 129172.
55 T. Yin, X. Meng, S. Wang, X. Yao, N. Liu and L. Shi, *Sep. Purif. Technol.*, 2022, **280**, 119634.
56 X. Li, J. Wang, Y. Guo, T. Zhu and W. Xu, *Chem. Eng. J.*, 2021, **411**, 128558.
57 S. Lu, Q. Liu, R. Han, J. Shi, M. Guo, C. Song, N. Ji, X. Lu and D. Ma, *Chem. Eng. J.*, 2021, **409**, 128194.
58 S. Lu, R. Han, H. Wang, C. Song, N. Ji, X. Lu, D. Ma and Q. Liu, *Chem. Eng. J.*, 2022, **448**, 137629.
59 M. Shafiei, M. S. Alivand, A. Rashidi, A. Samimi and D. Mohebbi-Kalhori, *Chem. Eng. J.*, 2018, **341**, 164–174.
60 Y. Pei, J. Qin, J. Wang and Y. Hu, *Sci. Total Environ.*, 2021, **790**, 148132.
61 L. Zhou, X. Zhang and Y. Chen, *Mater. Lett.*, 2017, **197**, 167–170.
62 R. Chen, Z. Yao, N. Han, X. Ma, L. Li, S. Liu, H. Sun and S. Wang, *ACS Omega*, 2020, **5**, 15402–15408.
63 D. P. Serrano, G. Calleja, J. A. Botas and F. J. Gutierrez, *Sep. Purif. Technol.*, 2007, **54**, 1–9.
64 A. Corma, *Chem. Rev.*, 1997, **97**, 2373–2420.
65 H. Kim, Y. Yoo, Y. Ahn, M. Park, K. Chue and M. Han, in *Adsorption Science & Technology*, World Scientific, 2003, pp. 286–290.
66 R. M. Barrer, *J. Chem. Soc.*, 1948, 127–132.
67 S. Brosillon, M.-H. Manero and J.-N. Foussard, *Environ. Sci. Technol.*, 2001, **35**, 3571–3575.
68 B. Wang, Y. Zhu, Q. Qin, H. Liu and J. Zhu, *Appl. Catal., A*, 2021, **611**, 117952.
69 E. Guvenc and M. G. Ahunbay, *J. Phys. Chem. C*, 2012, **116**, 21836–21843.
70 S. Bhatia, A. Z. Abdullah and C. T. Wong, *J. Hazard. Mater.*, 2009, **163**, 73–81.
71 S. P. Kremer, C. E. Kirschhock, M. Tielen, F. Collignon, P. J. Grobet, P. A. Jacobs and J. A. Martens, *Adv. Funct. Mater.*, 2002, **12**, 286–292.
72 Y. Zhang, L. Wang, L. He, B. Wu and Y. Cheng, *Chin. J. Chem. Eng.*, 2017, **11**, 5509–5514.
73 H. Liu, K. Wei and C. Long, *Chem. Eng. J.*, 2022, **442**, 136108.
74 D. Verboekend and J. Pérez-Ramírez, *Catal. Sci. Technol.*, 2011, **1**, 879–890.
75 J. S. Beck, J. C. Vartuli, W. J. Roth, M. E. Leonowicz, C. Kresge, K. Schmitt, C. Chu, D. H. Olson, E. Sheppard and S. McCullen, *J. Am. Chem. Soc.*, 1992, **114**, 10834–10843.
76 D. Zhao, J. Feng, Q. Huo, N. Melosh, G. H. Fredrickson, B. F. Chmelka and G. D. Stucky, *Science*, 1998, **279**, 548–552.

77 R. Ryoo, J. Kim, C. Ko and C. Shin, *J. Phys. Chem.*, 1996, **100**, 17718–17721.
78 Q. Huo, D. I. Margolese and G. D. Stucky, *Chem. Mater.*, 1996, **8**, 1147–1160.
79 Q. Yu, R. Zhuang, H. Yi, W. Gao, Y. Zhang and X. Tang, *Environ. Sci. Pollut. Res.*, 2022, **29**, 33595–33608.
80 H. Zhou, S. Gao, W. Zhang, Z. An and D. Chen, *RSC Adv.*, 2019, **9**, 7196–7202.
81 S. Liu, J. Chen, Y. Peng, F. Hu, K. Li, H. Song, X. Li, Y. Zhang and J. Li, *Chem. Eng. J.*, 2018, **334**, 191–197.
82 A. Feng, Y. Yu, L. Mi, Y. Cao, Y. Yu and L. Song, *Microporous Mesoporous Mater.*, 2019, **290**, 109646.
83 C. Zhao, X. Hu, C. Liu, D. Chen, J. Yun, X. Jiang, N. Wei, M. Li and Z. Chen, *J. Environ. Chem. Eng.*, 2022, **10**, 106868.
84 W. Yu, X. Wu, B. Cheng, T. Tao, X. Min, R. Mi, Z. Huang, M. Fang and Y. Liu, *Chem. – Eur. J.*, 2022, **28**, e202102787.
85 A. Feliczak-Guzik, *Microporous Mesoporous Mater.*, 2018, **259**, 33–45.
86 Q. Tang, W. Deng, D. Chen, D. Liu and L. Guo, *Dalton Trans.*, 2021, **50**, 16694–16702.
87 L. Han, L. Guo, S. Xue, Z. Wang, T. Lu, J. Xu, Y. Zhan and J. Wang, *Microporous Mesoporous Mater.*, 2021, **311**, 110676.
88 X. Jiang, C. Zhao, X. Hu, Z. Tong, J. Yun, N. Wei, K. Wang, C. Liu, Y. Zou and Z. Chen, *J. Chem. Technol. Biotechnol.*, 2022, **97**, 3498–3510.
89 O. M. Yaghi, G. Li and H. Li, *Nature*, 1995, **378**, 703–706.
90 H. Buser, D. Schwarzenbach, W. Petter and A. Ludi, *Inorg. Chem.*, 1977, **16**, 2704–2710.
91 O. Yaghi and H. Li, *J. Am. Chem. Soc.*, 1995, **117**, 10401–10402.
92 H. Li, M. Eddaoudi, M. O'Keeffe and O. M. Yaghi, *Nature*, 1999, **402**, 276–279.
93 D. Britt, D. Tranchemontagne and O. M. Yaghi, *Proc. Natl. Acad. Sci. U. S. A.*, 2008, **105**, 11623–11627.
94 L. Boudjema, J. Long, H. Petitjean, J. Larionova, Y. Guari, P. Trens and F. Salles, *Inorg. Chim. Acta*, 2020, **501**, 119316.
95 F. Xie, Y. Wang, L. Zhuo, D. Ning, N. Yan, J. Li, S. Chen and Z. Lu, *J. Hazard. Mater.*, 2021, **412**, 125260.
96 N. H. M. H. Tehrani, M. S. Alivand, A. Kamali, M. D. Esrafili, M. Shafiei-Alavijeh, R. Ahmadi, M. Samipoorgiri, O. Tavakoli and A. Rashidi, *J. Environ. Chem. Eng.*, 2023, **11**, 109558.
97 Q. Zhao, Q. Du, Y. Yang, Z. Zhao, J. Cheng, F. Bi, X. Shi, J. Xu and X. Zhang, *Chem. Eng. J.*, 2022, **433**, 134510.
98 K. Vellingiri, P. Kumar, A. Deep and K.-H. Kim, *Chem. Eng. J.*, 2017, **307**, 1116–1126.
99 J. Zhang, J. Shao, X. Zhang, G. Rao, P. Krivoshapkin, E. Krivoshapkina, H. Yang, S. Zhang and H. Chen, *Fuel*, 2023, **335**, 127013.
100 C. Dong, J. J. Yang, L. H. Xie, G. Cui, W. H. Fang and J. R. Li, *Nat. Commun.*, 2022, **13**, 4991.
101 S. H. Jhung, J. H. Lee, J. W. Yoon, C. Serre, G. Férey and J. S. Chang, *Adv. Mater.*, 2007, **19**, 121–124.
102 A. Jain, R. Balasubramanian and M. Srinivasan, *Chem. Eng. J.*, 2015, **273**, 622–629.
103 F. Gao, D.-L. Zhao, Y. Li and X.-G. Li, *J. Phys. Chem. Solids*, 2010, **71**, 444–447.
104 K. Yang, Q. Sun, F. Xue and D. Lin, *J. Hazard. Mater.*, 2011, **195**, 124–131.
105 X. Liu, C. Zhang, Z. Geng and M. Cai, *Microporous Mesoporous Mater.*, 2014, **194**, 60–65.
106 D. Crespo and R. T. Yang, *Ind. Eng. Chem. Res.*, 2006, **45**, 5524–5530.
107 M. Lillo-Ródenas, D. Cazorla-Amorós and A. Linares-Solano, *Carbon*, 2005, **43**, 1758–1767.
108 J.-H. Tsai, H.-M. Chiang, G.-Y. Huang and H.-L. Chiang, *J. Hazard. Mater.*, 2008, **154**, 1183–1191.
109 Y. An, Q. Fu, D. Zhang, Y. Wang and Z. Tang, *Chemosphere*, 2019, **227**, 9–16.
110 X. Wang, H. Cheng, G. Ye, J. Fan, F. Yao, Y. Wang, Y. Jiao, W. Zhu, H. Huang and D. Ye, *Chemosphere*, 2022, **287**, 131995.
111 H. Zhao, Z. Tang, M. He, X. Yang, S. Lai, K. An, S. Han, Z. Qu, W. Zhou and Z. Wang, *Sci. Total Environ.*, 2023, **863**, 160772.
112 E. P. Hessou, H. Jabraoui, M. T. A. K. Hounguè, J.-B. Mensah, M. Pastore and M. Badawi, *Z. Kristallogr. – Cryst. Mater.*, 2019, **234**, 469–482.
113 S. Kang, J. Ma, Q. Wu and H. Deng, *J. Chem. Eng. Data*, 2018, **63**, 2211–2218.
114 B. Siu, A. R. Chowdhury, Z. Yan, S. M. Humphrey and T. Hutter, *Coord. Chem. Rev.*, 2023, **485**, 215119.
115 Y. Xie, S. Lyu, Y. Zhang and C. Cai, *Materials*, 2022, **15**, 7727.
116 S. Sharafinia, A. Rashidi and M. D. Esrafili, *J. Environ. Chem. Eng.*, 2022, **10**, 108528.
117 F. Meng, M. Song, Y. Wei and Y. Wang, *Environ. Sci. Pollut. Res.*, 2019, **26**, 7195–7204.
118 X. Guo, X. Li, G. Gan, L. Wang, S. Fan, P. Wang, M. O. Tadé and S. Liu, *ACS Appl. Mater. Interfaces*, 2021, **13**, 56510–56518.